All-electron local and gradient-corrected density-functional calculations of Na_n dipole polarizabilities for n=1–6

Jingang Guan, Mark E. Casida, Andreas M. Köster, and Dennis R. Salahub
Département de Chimie, Université de Montréal, Montréal, Québec, Canada H3C 3J7
(Received 28 November 1994)

Sodium clusters represent an experimentally accessible and seemingly simple system for studying the size dependence of the optical properties of metal clusters. Nevertheless, with the exception of the atom and dimer, previous *ab initio* calculations have either been restricted to correlated calculations in which pseudopotentials were used in order to reduce sodium to an effective one-electron atom or correlation effects were entirely neglected. The present study presents the results of correlated all-electron density-functional calculations of sodium-cluster dipole polarizabilities for clusters through the hexamer. In particular, polarizabilities were calculated at the local-density-approximation- (LDA-) optimized geometries using the LDA functional, with the Perdew-Wang 1986 exchange plus the Perdew 1986 correlation (PW86x+P86c) gradient corrections, and with the Becke 1988 exchange plus the Perdew 1986 correlation (B88x+P86c) gradient corrections. The results are compared with the available experimental and *ab initio* theoretical values. Of the three exchange-correlation functionals presented in this paper, the mean polarizabilities calculated using the B88x+P86c functional are in best agreement with the experimental values, with discrepancies between theory and experiment of only 3.5% for the atom and 5% for the dimer. Differences between the experimental and B88x+P86c optimized dimer and trimer geometries are also significantly smaller than in the LDA case. However, there is little difference between mean polarizabilities calculated at the LDA-optimized, B88x+P86c optimized, and experimental geometries. In particular, this cannot explain the 11–22 % discrepancies found here between the experimental polarizabilities for the trimer and higher-order clusters and those calculated at the LDA-optimized geometries using the B88x+P86c functional. It is suggested that molecular motion may need to be taken into account before a completely satisfactory explanation of the experimental polarizabilities of these floppy molecules can be given.

I. INTRODUCTION

The polarizabilities of metal clusters have been the focus of considerable attention in recent years. This attention stems partly from the long-standing interest in the size dependence of optical properties of small particles[1,2] as an aid to the understanding and engineering of novel materials,[3] and partly from the relative ease of measurement of cluster polarizabilities[4–6] as one structural clue in an area where direct experimental clues to cluster geometries are few and far between. Of course, both the prediction of optical properties and the extraction of structural information from polarizability measurements presupposes an adequate theoretical understanding for quantitative predictions of cluster polarizabilities. We will focus on the electronic component of the polarizability, which is expected to be the dominant contribution to the measured quantity.

Homonuclear alkali metal clusters are often considered to be the simplest metal clusters because they have only a single valence electron. In fact, sodium clusters have become a prototype system for understanding size effects in metal clusters. A hierarchy of models has emerged from these studies which can be used to understand cluster properties in an increasingly quantitative fashion. We begin with a brief review of the hierarchy of models that have been used to describe sodium-cluster polarizabilities.

There are several popular models for sodium-cluster polarizabilities in which each N-atom cluster is treated as a sphere of radius R determined from the number density of atoms, ρ, of bulk sodium by

$$\frac{4\pi}{3}R^3 = \frac{N}{\rho}. \tag{1.1}$$

The simplest and oldest model is that of a classical conducting sphere, of radius $a = R$, whose polarizability can be shown[7] to be

$$\bar{\alpha} = a^3 = \frac{3N}{4\pi\rho}. \tag{1.2}$$

This is, of course, exact in the limit of a macroscopic spherical cluster. Bulk alkali metals are often analyzed in terms of the free electron model,[8] so it is not surprising that the next and most common level of approximation is the jellium sphere,[9–15] a quantum mechanical model in which there are N electrons and a sphere with a uniform

charge of $+N$. Part of the difference between this quantum mechanical jellium sphere model and the classical sphere model stems from the fact that the quantum mechanical electron density extends beyond the radius of the classical sphere, with the result that the sphere is effectively larger. This simple size effect can be incorporated into the classical formula (1.2), in a "spillout model,"[9,16] by taking the radius of the sphere to be $a = R + \delta$, where the value of δ is obtained empirically.[9] The polarizability is then given by

$$\bar{\alpha} = N\left[\left(\frac{3}{4\pi\rho}\right)^{1/3} + \frac{\delta}{N^{1/3}}\right]^3 . \tag{1.3}$$

However, the spillout model cannot account for the more interesting quantum mechanical effects. Deviations of jellium sphere polarizabities from formula (1.3) represent "true" quantum effects. These can be understood in part in terms of the "shell model,"[17,16] which predicts clusters with $N = 2, 8, 18, 20, \ldots$ to have particularly stable electron configurations. (See Refs. 18 and 19 for detailed reviews of the successes and failures of the shell and jellium sphere models for explaining a variety of properties of simple metal clusters.)

While spherical models may be useful in gaining a qualitative understanding of the mean polarizabilities of large sodium clusters, they are obviously useless for predictions of polarizability anisotropies. Furthermore, small sodium clusters are not particularly spherical and even a description of the mean polarizability should take into account the molecular nature of the cluster ("atomic effects"). While some attempt to study atomic effects has been made by packing jellium spheres whose cores repel each other according to a Z^2/r law[20] or by using a spherical average of atomic core potentials,[15] a full *ab initio* solution of the molecular quantum mechanical problem seems more appropriate.

Moullet and co-workers[21–24] have made some progress in this direction, in a series of density-functional studies. These results are in markedly better agreement with the experimental polarizabilities measured by Knight *et al.*[4] than are the predictions of the jellium model, and represent a first serious step towards a more profound molecular understanding of factors governing polarizabilities of small sodium clusters. However, these studies use effective core potentials (ECP's) to reduce sodium to an effective one-electron atom.

When one considers that, in sodium, the core represents the vast majority of the electron density, and that it is the total charge density, not only the valence electrons, which is involved in the response to an applied electric field, the use of a frozen core approximation, in which the ECP is not polarizable, for the calculation of cluster polarizabilities should be examined carefully. This is particularly so in the light of experience calculating the polarizability of the sodium atom using traditional quantum chemistry methods. All-electron Hartree-Fock calculations give a mean polarizabililty of 190.9 bohr^3.[25] The importance of electron correlation effects is immediately obvious when this is compared with the experimental value of 159.3 ± 3.4 bohr^3.[26] Attempts to improve on this by introducing correlation effects, but while keeping the frozen core approximation, lead to essentially no change in the mean polarizabilities[27–29] for the obvious reason that there is only one electron outside the frozen core. In contrast, including core-valence correlation effects leads to a value of 165.2 bohr^3,[27] in markedly better agreement with experiment. These experiences underline the dangers of freezing the L shell when calculating sodium-cluster polarizabilities by traditional *ab initio* methods. A (less precise) alternative to all-electron calculations is to simulate the effects of core-core and core-valence correlation by use of a core polarization potential,[30] but this requires validation against the results of all-electron calculations.

Since density-functional theory accounts for electron correlation effects in a very different way than does conventional *ab initio* theory, ECP's may still be viable for density-functional calculations of sodium-cluster polarizabilities, especially if polarizable ECP's[31] are used. Although this would be very useful for large clusters, such ECP's should first be carefully checked for this purpose against all-electron calculations. This is especially true if one is interested in calculating sensitive quantities such as polarizability anisotropies or taking polarizability derivatives to get hyperpolarizabilities. It should be emphasized that, although the comparison of the ECP density-functional mean polarizabilities of Moullet and co-workers[21–24] with experiment are quite encouraging, the calculations using ECP's should really be tested against the all-electron calculations they are intended to model, since other factors, such as vibrational effects and experimental errors, can enter into the comparison with experiment.

Other than for the atom,[27] correlated all-electron calculations of sodium-cluster polarizabilities are very rare. Sadlej and Urban have recently performed high-level correlated all-electron calculations of the polarizability of the dimer in which only the innermost (K) shell is frozen;[32] however, we are unaware of any studies of polarizabilities of comparable rigor for the trimer and above. Given the efficiency of state-of-the-art molecular density-functional programs, such studies are quite feasible for the first several clusters. In this paper, we present all-electron calculations of both the mean polarizability and polarizability anisotropy for sodium clusters up through the hexamer. Although polarizabilities are among the properties that can be calculated in principle exactly in density-functional theory in the limit of an exact exchange-correlation functional, this functional must be approximated in practice. Since the results of density-functional calculations of polarizabilities depend upon the particular choice of approximate functional used, several functionals have been considered here.

This paper is organized in the following fashion. Our theoretical method and the technical details of our computations are described in the next section. Our results are reported in Sec. III and our conclusions are summarized in Sec. IV. Unless otherwise indicated, hartree atomic units ($\hbar = m = e = 1$) are used throughout.

II. THEORETICAL METHODS

A. Density-functional theory

The conceptual basis and basic equations of density-functional theory are too well known to need review here. Suffice it to say that Kohn-Sham density-functional theory[33] (KS DFT) is a formally exact method in which the ground-state total energy and charge density, $n(\vec{r})$, of a system of N interacting electrons in a local external potential, $v_{\rm ext}(\vec{r})$, are determined by minimizing an energy expression with respect to a set of fictitious orthonormal orbitals whose charge densities sum to the exact charge density. This energy expression contains a formally exact but unknown exchange-correlation energy term, $E_{\rm xc}[n^\uparrow, n^\downarrow]$, which is a functional of the spin up, $n^\uparrow$, and spin down, $n^\downarrow$, charge densities. It must be approximated in practice. A detailed review of fundamental density-functional theory can be found in Refs. 34–36.

Our calculations were carried out at the all-electron level using the density-functional program deMon.[37] No effective or model core potentials have been used and the core has been left unfrozen. Several choices of exchange-correlation functional are available in deMon. The simplest and most widely used approximation in the density-functional literature is the local-density approximation (LDA),

$$E_{\rm xc}^{\rm LDA}[n^\uparrow, n^\downarrow] = \int n(\vec{r}) \epsilon_{\rm xc}(n^\uparrow(\vec{r}), n^\downarrow(\vec{r}))\, d\vec{r}. \qquad (2.1)$$

Here $\epsilon_{\rm xc}(n^\uparrow, n^\downarrow)$ is the exchange-correlation energy density for a homogeneous electron gas with spin-up electron density $n^\uparrow$ and spin-down electron density $n^\downarrow$. The exchange part of the exchange-correlation energy density for the homogeneous electron gas is known exactly and leads to the exchange-only local-density approximation (LDAx),

$$E_x^{\rm LDA}[n^\uparrow, n^\downarrow] = 2^{1/3} \sum_\sigma^{\rm spin} \left[-\frac{3}{4} \left(\frac{3}{\pi} \right)^{1/3} \right] \int [n^\sigma(\vec{r})]^{4/3}\, d\vec{r}. \qquad (2.2)$$

However, no closed form is known for the correlation energy density of the homogenous electron gas. Instead, we use the parametrization of Vosko, Wilk, and Nusair,[38] which is based upon the Monte Carlo calculations of Ceperley and Alder.[39]

Although the LDA is an adequate starting point for many purposes, it neglects any dependence on the gradients of the density, and is therefore only rigorously justified in the limit of slowly varying densities. One way to take into account inhomogeneities in the electron density is through the use of gradient-corrected functionals (GCF's),

$$E_{\rm xc}^{\rm GCF}[n^\uparrow, n^\downarrow] = \int n(\vec{r}) \epsilon_{\rm xc}(n^\uparrow(\vec{r}), n^\downarrow(\vec{r}), \vec{\nabla} n^\uparrow(\vec{r}), \vec{\nabla} n^\downarrow(\vec{r}))\, d\vec{r}. \qquad (2.3)$$

Two well-known exchange-only GCF's are used in the present work, namely, the 1988 GCF of Becke[40] (B88x) and the 1986 GCF of Perdew and Wang[41] (PW86x). The B88x GCF was designed to reproduce the correct $(-1/r)$ asymptotic behavior of the exchange energy density $\epsilon_{\rm x}(\vec{r})$. Although the PW86x GCF does not have this property, it does satisfy the conditions that the exchange hole be everywhere negative and represents a deficit of exactly one electron. Correlation has been treated using the 1986 GCF of Perdew[42] (P86c), which is ultimately based upon the wave-vector analysis of Langreth and Mehl,[43] but which improves upon this by taking into account uniform-gas and inhomogeneity effects beyond the random-phase approximation and making a more natural separation between exchange and correlation.

The orbital basis sets used in the present work are of the same type used in conventional *ab initio* electronic structure work. This is possible because deMon belongs to the linear-combination-of-Gaussian-type-orbitals family of density-functional programs in which the Kohn-Sham molecular orbitals are expanded in a basis of Gaussian-type orbitals (GTO's). This allows both the programmers and users of deMon to take advantage of the wealth of experience accumulated during the development and application of GTO-based Hartree-Fock (HF) codes. In particular, the same terminology may be used for describing orbital basis sets as is current for conventional *ab initio* methods using GTO basis sets.[44]

An important distinction between density-functional theory codes and conventional *ab initio* codes is the use of a grid to treat exchange-correlation terms. The way the grid is used in deMon is linked to a second difference from conventional *ab initio* codes. This is the use of two GTO auxiliary basis sets. The charge density is approximated by a purely analytic fit to an expansion in a so-called charge density auxiliary basis set of M functions. This allows the number of Coulomb integrals which must be evaluated to be reduced from N^4 to MN^2, where N is the size of the orbital basis set used in the calculation. The second auxiliary basis set is used to help evaluate integrals involving the exchange-correlation potentials $[v_{\rm xc}^\sigma(\vec{r})]$ and the exchange-correlation energy density $[\epsilon_{\rm xc}(\vec{r})]$. These integrals cannot be evaluated analytically. Instead, the exchange-correlation potentials and energy density are approximated by a least-squares fit to an expansion in a so-called exchange-correlation auxiliary basis set. A grid is used during the fitting procedure for the exchange-correlation potentials and energy density, but, once the fitting is completed, any exchange-correlation integrals can then be evaluated analytically. Experience shows that most results are rather insensitive to the precise nature of the auxiliary basis set.

The parameters used in our calculations tend to be tighter than those normally used in deMon calculations. This is necessary for two reasons. The first is that these clusters tend to be relatively floppy, so that small numerical errors can sometimes lead to qualitatively incorrect geometries unless proper care is taken. This is the case for the tetramer discussed below. The second reason for using tighter parameters is our own experience that such parameters are needed for well-converged polarizability

calculations. The choice of basis set and method for the polarizability calculations are discussed in detail in a separate subsection below.

The geometry optimizations reported here were carried out at the B88x+P86c level for the dimer and trimer as well as at the LDAxc level for all the clusters. Although the B88x+P86c functional will be shown to lead to geometries in better agreement with experiment than does the simple LDAxc, it will also be shown that the difference in the optimized geometry due to the choice of functional has only a very minor effect on the calculated polarizability. All geometry optimizations used the double-zeta valence plus polarization (DZVP) quality orbital basis set and the (5,4;5,4) auxiliary basis sets from the deMon basis set library. Convergence during the self-consistent field steps is attained when both the energy and charge density fitting coefficients stop changing. The convergence criteria used here for both the geometry optimizations and polarizability calculations were 10^{-8} hartree for the energy and 10^{-7} a.u. for the charge density fitting coefficients. Geometries were optimized using a step size of 0.05 bohr and are converged to a gradient of less than 10^{-5} a.u. in absolute value. The fine random grid was used which consists of a 32-point radial grid and a 26-point angular grid for a total of 832 grid points per atom. This grid proved to be insufficient for optimizing the geometry of the tetramer, which has a very soft in-plane vibrational mode indicating a flat potential energy along that normal mode coordinate. In order to deal with this problem, deMon was modified to permit the user to expand the number of radial grid points, while still keeping the Gauss-Legendre distribution and weighting scheme used in the standard version of the program. The final geometry for Na_4 was well converged using a 128-point radial grid and a 194-point angular grid for a total of 24 832 grid points per atom.

B. Polarizability calculations

The static dipole moment, polarizability, and hyperpolarizability may be defined in terms of a Taylor expansion of the molecular energy in the (x, y, and z) components of a uniform electric field $\vec{F}$,

$$E(\vec{F}) = E(\vec{0}) - \sum_i \mu_i F_i - \frac{1}{2}\sum_{ij} \alpha_{ij} F_i F_j - \frac{1}{6}\sum_{ijk} \beta_{ijk} F_i F_j F_k + \cdots , \tag{2.4}$$

where $E(\vec{0})$ is the total energy of the molecule in the absence of the electric field, and the quantities

$$\mu_i = -\left[\frac{\partial E}{\partial F_i}\right]_{\vec{F}=\vec{0}} , \tag{2.5}$$

$$\alpha_{ij} = -\left[\frac{\partial^2 E}{\partial F_i \partial F_j}\right]_{\vec{F}=\vec{0}} , \tag{2.6}$$

$$\beta_{ijk} = -\left[\frac{\partial^3 E}{\partial F_i \partial F_j \partial F_k}\right]_{\vec{F}=\vec{0}} , \tag{2.7}$$

are, respectively, the permanent dipole moment, the dipole polarizability, and the first dipole hyperpolarizability. A technical point is that even a small uniform electric field is enough to make the potential binding the electrons infinitely negative in the direction opposing the applied field. However, the electron states, while no longer technically bound, are still long lived since the barrier to dissociation is significant for sufficiently small applied fields and the lifetime of these quasibound states becomes infinite in the limit of an infinitely small applied field. Thus Eq. (2.4) is rigorously valid for either infinitesimally small applied fields or for finite systems, say, in a box. The finite basis set calculations reported here are essentially of the latter nature. However, explicit comparisons of, say, coupled Hartree-Fock calculations using infinitesimally small fields (i.e., analytic derivatives) and finite field Hartree-Fock calculations show that identical polarizabilities are obtained in the two approaches.[45]

The tensors μ_i, α_{ij}, β_{ijk}, etc. depend upon the choice of coordinate system. Since this is inconvenient when comparing with experiment or other theoretical calculations, results are often reported in terms of rotational invariants. Traditional choices for polarizability invariants are the mean polarizability,

$$\bar{\alpha} = \frac{1}{3}\mathrm{tr}\,\boldsymbol{\alpha} \tag{2.8}$$

and the polarizability anisotropy,

$$(\Delta\alpha)^2 = \frac{1}{2}\left[3\mathrm{tr}\,(\boldsymbol{\alpha}^2) - (\mathrm{tr}\,\boldsymbol{\alpha})^2\right] . \tag{2.9}$$

Alternatively, the Hellmann-Feynman theorem can be used to calculate the field-induced dipole moment $\Delta\vec{\mu}(\vec{F}) = \vec{\mu}(\vec{F}) - \vec{\mu}$ from the electron charge density $n(\vec{r};\vec{F})$ in the presence of the electric field,

$$\mu_i(\vec{F}) = -\int r_i n(\vec{r};\vec{F})\, d\vec{r} + \sum_I^{\text{nuclei}} Z_I R_{I,i} , \tag{2.10}$$

where Z_I and $R_{I,i}$ are, respectively, the charge on the Ith nucleus and the ith component of its position vector. Note that this expression is invariant under translations of the coordinate system for neutral molecules. Evidently,

$$\mu_i(\vec{F}) = \mu_i + \sum_j \alpha_{ij} F_j + \frac{1}{2}\sum_{j,k} \beta_{ijk} F_j F_k + \cdots , \tag{2.11}$$

which shows that the polarizability and hyperpolarizability can equivalently be defined in terms of the response of the field-induced dipole moment.

Our polarizability calculations were carried out using the finite field method in which the derivative of the induced dipole moment is obtained by the three-point finite difference formula,

$$\alpha_{ij} = \frac{\mu_j(+\vec{F}_i) - \mu_j(-\vec{F}_i)}{2F_i}, \tag{2.12}$$

and deMon's default field step size of 0.0005 a.u. Here $\vec{F}_i$ is a uniform electric field in the i direction. Since

TABLE I. Orbital basis set used for present polarizability calculations. Note that deMon uses six Cartesian d functions.

Sodium DZVP+ basis set	
Exponent	Contraction coefficients
1S	
9911.9960000000	0.0019504590
1487.4550000000	0.0149171200
337.9539000000	0.0734165800
94.9139500000	0.2456910000
30.3415000000	0.4795611000
10.1908400000	0.3337213000
2S	
21.2296500000	0.0823028800
1.9804180000	-0.5608480000
0.6188824000	-0.5224378000
3S	
0.6991738000	0.0920975500
0.0618270500	-0.6708252000
4S	
0.0237274100	1.0000000000
1P	
73.0853100000	0.0167176300
16.8645600000	0.1065395000
5.0553910000	0.3242217000
1.5920210000	0.4891362000
2P	
0.4702690000	1.0000000000
3P	
0.0647000000	1.0000000000
4P (FIP)	
0.0280000000	1.0000000000
1D	
0.1169000000	1.0000000000

our objective is accurate Kohn-Sham polarizabilities and given previous concerns with the numerical method used for calculating hyperpolarizabilities,[45] the accuracy of the three-point finite difference formula and possible numerical contamination from hyperpolarizability terms were tested by several polarizability calculations using the polynomial fitting method, in which the coefficients in Eq. (2.11) are determined by a least-squares fitting procedure.[45] These results indicated that the finite difference method was sufficient for polarizability calculations (e.g., the mean polarizability of the dimer was 226.24 bohr^3 by the finite difference method and 226.17 bohr^3 from a least-squares fit to a sixth-order polynomial), so the calculations reported here were carried out using the less expensive finite difference method.

The same grid, auxiliary basis sets, and convergence criteria were used in the polarizability calculations as in the geometry optimizations. However, the effect of changing the auxiliary basis set was checked by carrying out calculations on the trimer with both the (5,4;5,4) and the (6,5;6,5) auxiliary basis sets from the deMon library. The mean polarizability calculated with the former was 371.27 bohr^3 and was 370.48 bohr^3 with the latter, indicating that the (5,4;5,4) auxiliary basis set used throughout the present work is indeed adequate.

The experience[45,46] with density-functional and Hartree-Fock polarizability calculations is that "medium size" basis sets, such as the DZVP basis set, need to be extended by an additional set of diffuse polarization functions. This is reasonable because such basis sets were designed to describe the molecule in the absence of an applied electric field. A simple perturbation analysis[47] indicates that diffuse functions of at least one higher angular

TABLE II. Other orbital basis sets considered in the present study and mean polarizabilities calculated with these basis sets. See also Fig. 2. The field-induced polarization (FIP) function exponents were optimized for the atom using the LDAxc functional. The field strengths used were 0.025 a.u. when the exponents were determined by minimizing the energy and 0.0005 a.u. when the exponents were determined by maximizing the polarizability.

Basis	Size[a]	$\bar{\alpha}$ (bohr^3)			Description
		atom	dimer	trimer	
			Substrate basis set		
A (DZVP)	22	95.68	189.78	312.27	Valence double-zeta plus polarization[b]
			FIPs optimized by minimizing the energy		
B	22	134.54	219.59	365.54	Basis A with outermost p function reoptimized
D	25	136.09	225.20	375.77	Basis A + p-type FIP function
			FIPs optimized by maximizing the polarizability		
C	22	139.11	218.20	359.36	Basis set A with outermost p function reoptimized
E (DZVP+)	25	140.12	226.24	371.27	Basis A + p-type FIP function
F	28	140.02	226.30	371.68	Basis E + 2nd p-type FIP function
G	28	95.69	190.11	349.95	Basis A + d-type FIP function
H	31	140.47	226.69	376.55	Basis E + d-type FIP function
			Experimental mean polarizability[c]		
		159.27±3.37	255.78±8.10	471.06±16.20	

[a]Number of contractions.
[b](6321/411*/1+).
[c]Calculated from the measurements of relative polarizabilities of Knight *et al.* (Ref. 4) and the absolute measurement of the atomic polarizability by Molof *et al.* (26).

momentum beyond that in a minimal basis are needed for the calculations of polarizability. These are referred to as field-induced polarization (FIP) functions and should not be confused with the much tighter polarization functions already included in (for example) the DZVP basis set, which are intended to describe the polarization of atomic orbitals upon bonding. The number of these additional FIP functions can be substantially reduced by careful choice of the exponent of the FIP functions. They could be chosen to be a function of field strength,[48–50] or on the basis of a perturbative analysis of field-induced changes in the orbitals of hydrogenic atoms,[47] or by maximizing the polarizability of the atom.[51,52]

Our final choice of FIP functions were optimized by maximizing the polarizability of the sodium atom using the LDAxc functional and a field strength of 0.0005 a.u. The justification for this method rests on the fact that the total energy for the atom in the presence of an applied field of strength F is given by

$$E(F) = E(0) - \frac{1}{2}\bar{\alpha}F^2 + O(F^4)\,, \tag{2.13}$$

where the direction of the applied field is irrelevant. If the substrate basis set is assumed adequate for the field-free calculation in the sense that addition of the FIP leaves $E(0)$ essentially unchanged and F is adequately small, minimizing $E(F)$ and maximizing $\bar{\alpha}$ are equivalent. The basis set optimized in this way is given in Table I.

Variations on this procedure were also considered and are summarized in Table II. Basis set C is a partial re-optimization of the substrate basis set, without adding additional basis functions, by maximizing the polarizability of the atom. Basis sets E, F, G, and H were made from the substrate basis set by adding orbitals with exponents chosen to maximize the polarizability of the atom. Basis sets B and D are analogous to basis sets C and E except that the LDAxc energy has been minimized in the presence of a 0.025 a.u. electric field. Differences in the cluster polarizabilities calculated with these basis sets and our final choice of basis set E are discussed in Sec. III.

III. RESULTS

A. Geometries

The structures used in our polarizability calculations have been obtained by optimizations at the LDAxc/DZVP level beginning with minimum energy geometries already reported in the literature.[53] Our optimized geometries are shown in Fig. 1. Comparison of minimum energy and zero gradient criteria for the dimer indicates that the numerical precision of deMon for the Na_2 bond length at this level is about ± 0.03 bohr. This number should be compared to the same estimate for the more strongly bound molecule N_2, where the numerical imprecision in the bond length is negligible. No significant change in the optimized geometries was observed when calculations were performed at the LDAxc/DZVP+ level. The final LDAxc-optimized bond length is within 0.04 bohr of that obtained from entirely numerical, basis-set-free calculations with the same functional.[54,55]

The optimized structures in Fig. 1 can be compared with the available experimental and high-quality theoretical cluster geometries. Direct experimental informa-

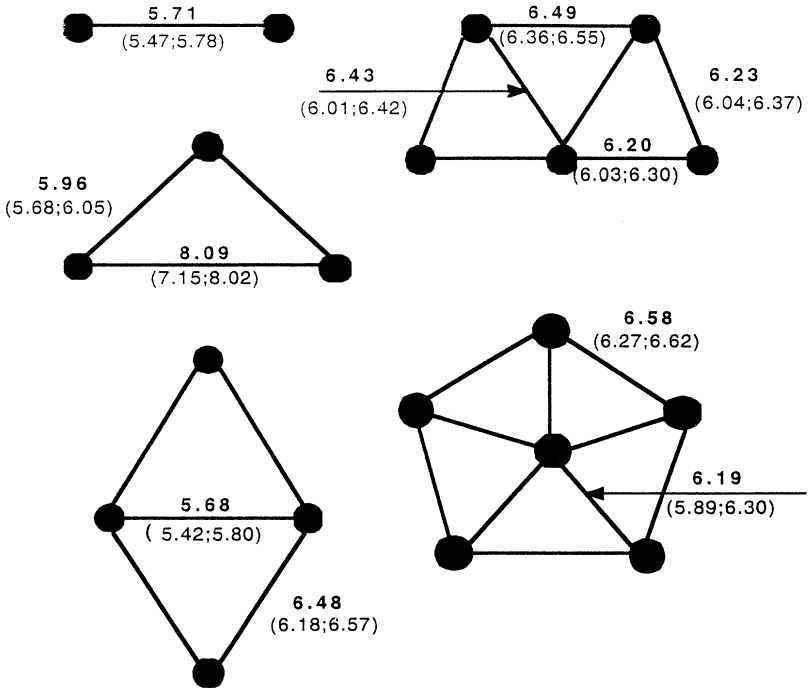

FIG. 1. LDAxc/DZVP-optimized cluster geometries used in this work. Clusters with an even number of atoms have singlet ground states. Those with an odd number of atoms have doublet ground states. All structures are planar except for Na_6, in which the central atom is out of the plane. All distances are in bohr. Distances which are not shown can be determined by symmetry and comparison with distances which are shown. The numbers shown in parentheses are the internuclear distances obtained by Moullet *et al.* using the BHS *ab initio* ECP (first number) and the brd semiempirical ECP (second number). See text for additional details.

TABLE III. Equilibrium bond length in bohr of singlet Na_2 obtained by various methods.

Bond length	Method	Basis	Reference
Effective core potential density-functional theory			
5.47	BHS LDAxc	[3*s*3*p*]	21
5.78	brd LDAxc	[3*s*3*p*]	21
All-electron density-functional theory			
5.67	LDAxc	none[a]	54
5.667	LDAxc	none[a]	55
5.71	LDAxc	DZVP	present work
5.71	LDAxc	DZVP+	present work
5.86	B88x+P86c	DZVP+	present work
5.84	B88x+P86c	H[b]	present work
All-electron conventional *ab initio*			
5.99	HF	[7*s*4*p*1*d*]	63
5.815	MRDCI	[7*s*4*p*1*d*]	64
Experimental value			
5.818			57

[a]Fully numerical basis-set-free calculation.
[b]See Table II.

tion about cluster geometries is very rare and sodium clusters are no exception in this regard. Although the dimer geometry has been known experimentally for some time,[56,57] the trimer geometry has only been recently determined experimentally[58] by optical double resonance spectroscopy. No quantitative experimental geometries appear to be available for the tetramer and higher clusters. In contrast, theoretical information about sodium-cluster geometries is relatively plentiful. Sodium-cluster geometries through the hexamer have been optimized at the effective core potential LDAxc level,[53,20] all-electron Hartree-Fock level,[59] ECP configuration interaction (CI) level,[59,60] and fourth-order Møller-Plesset perturbation theory (MP4) level,[61] to mention only a few of the many studies of minimum energy sodium-cluster geometries. There is broad general agreement about the topology of the minimum energy geometry for all the clusters except the hexamer, where, in addition to the C_{5v} structure in Fig. 1, there are also nearly degenerate D_{3h} and C_{2v} structures.[62] Taken together, these studies indicate that sodium-cluster internuclear distances tend to be too short at the LDAxc level and too long at the HF level. Addition of post-HF correlation effects result in shorter internuclear distances in better agreement with experiment. These trends are illustrated in Tables III and IV, where our own results for the dimer and trimer are compared with the available experimental geometries and with theoretical geometries obtained by other methods. In the dimer case, our LDAxc bond length is 0.1 bohr too short while the HF bond length of Ref. 63 is 0.17 bohr too long in comparison to experiment. In the trimer case, the short side of the triangle is too short in comparison with experiment by 0.17 bohr in our LDAxc calculations and too long by 0.22 bohr in the HF calculations of Ref. 63. The long side of the triangle is too long compared to experiment by 0.20 bohr in our LDAxc calculations and too long by 0.64 bohr in the HF calculations of Ref. 63. The magnitude of these errors in LDAxc bond lengths should be kept in mind when considering polarizabilities calculated with these geometries.

Also shown in Tables III and IV are geometries that we have optimized at the B88x+P86c level and CI calculations from Refs. 64 and 65. The B88x+P86c geometries have longer bond lengths and are in better agreement with the experimental geometries than are the LDAxc geometries. Similarly, the CI geometries have shorter bond lengths and are in better agreement with the experimental geometries than are the HF geometries. However, we will show that these differences between optimized geometries have only a minor effect on calculated polarizabilities.

Our all-electron LDAxc results can also be compared with sodium-cluster geometries optimized at the LDAxc level using ECP's. We will confine our discussion to the geometries used by Moullet and co-workers[21–24] in their calculations of sodium-cluster polarizabilities. They considered both an *ab initio* ECP due to Bachelet, Hamann,

TABLE IV. Equilibrium distances in bohr and triangle area in bohr^2 for doublet Na_3 obtained by various methods. Note that the equilibrium geometry is that of an obtuse C_{2v} triangle.

Short side	Long side	Area	Method	Basis	Reference
Effective core potential density-functional theory					
5.68	7.15	15.8	BHS LDAxc	[3*s*3*p*]	21
6.05	8.02	18.2	brd LDAxc	[3*s*3*p*]	21
All-electron density-functional theory					
5.96	8.09	17.7	LDAxc	DZVP	present work
5.96	8.06	17.7	LDAxc	DZVP+	present work
6.12	8.50	18.7	B88x+P86c	DZVP+	present work
6.13	8.50	18.8	B88x+P86c	H[a]	present work
All-electron conventional *ab initio*					
6.46	9.05	20.9	HF	[3*s*2*p*]	59
6.35	8.50	20.1	HF	[7*s*4*p*1*d*]	63
6.26	7.46	18.8	MRSDCI	[6*s*4*p*1*d*]	65
Experimental value					
6.130	7.856	18.48	optical double resonance		58

[a]See Table II.

and Schlüter[66] (BHS), which is intended to give results as close as possible to what would be obtained from all-electron LDAxc calculations, and the semiempirical ECP of Bardsley[67] (brd), which was parametrized by fitting the experimental spectrum of the atom. The LDAxc-optimized geometries obtained using these ECP's are shown in parentheses in Fig. 1. These numbers illustrate the difficulties with using ECP's for precise work because it is the semiempirical brd ECP which best reproduces the all-electron results, rather than the BHS ECP, which was specifically intended to mimic the all-electron calculation.

B. Polarizabilities

Mean polarizabilities calculated at the LDAxc level using various basis sets and the all-electron LDAxc geometries from Fig. 1 are shown in Table II and Fig. 2. Since the substrate DZVP basis set has been kept fixed, the mean polarizabilities shown are primarily an indication of convergence with respect to augmentations with field-induced polarization functions. It is apparent from Table II and Fig. 2 that the deMon library basis set DZVP is insufficient for polarizability calculations. Reoptimization of the exponent of the outermost set of p-type functions either by the minimum energy criterion (basis B) or the maximum polarizability criterion (basis C) improves the calculated mean polarizabilities of the clusters considerably in comparison with experiment, but the replacement of a p function chosen for its ability to describe bonding with one to describe polarization in an external field is not recommended. Instead, it is better to add an additional set of p-type FIP basis functions with exponents optimized either by the minimum energy criterion (basis D) or by the maximum polarizability criterion (basis E). The maximum absolute difference between the mean polarizabilities calculated using FIP's constructed from the minimum energy and maximum polarizability criterion is 3.2%. Consideration of the effect of adding still more FIP's to the basis set was restricted to FIP's constructed from the maximum polarizability criterion. Neither additional p-type FIP functions (basis F) nor additional d-type FIP functions (bases G and H) have a very significant effect on the calculated mean polarizabilities, so we settled on basis set E (DZVP+) for the polarizability calculations reported here. An independent test of the quality of the DZVP+ basis set for calculating polarizabilities was made by performing calculations of the atomic and diatomic mean polarizabilities using the more extensive basis set of Sadlej and Urban[25] and yielded only insignificant changes. (The atomic LDAxc mean polarizabiilty is 141.19 bohr^3 with the Sadlej-Urban basis set, compared with 140.12 bohr^3 using the DZVP+ basis set; the diatomic LDAxc mean polarizability is 227.28 bohr^3 with the Sadlej-Urban basis set, compared with 226.24 bohr^3 using the DZVP+ basis set; and the triatomic mean polarizability is 379.80 bohr^3 with the Sadlej-Urban basis set, compared with 371.27 bohr^3 using the DZVP+ basis set.) Thus we are relatively confident about the quality of the DZVP+ basis set for calculating polarizabilities. Moreover, it is interesting to note that, while there is a 30% increase in the polarizability of the atom in going from the DZVP to the DZVP+ basis set, the percent improvement actually decreases as the size of the cluster increases, presumably because the importance of the FIP functions is diminished by the availability of basis functions on other sites ("basis set borrowing"). Table V shows the convergence of the cluster polarizability anisotropies as a function of basis set. This property is more sensitive to choice of basis set than is the mean polarizability. Nevertheless, the DZVP+ basis set appears to be reasonably well converged for polarizability anisotropies. The rest of the discussion of our results will be confined to those obtained with the DZVP+ basis set.

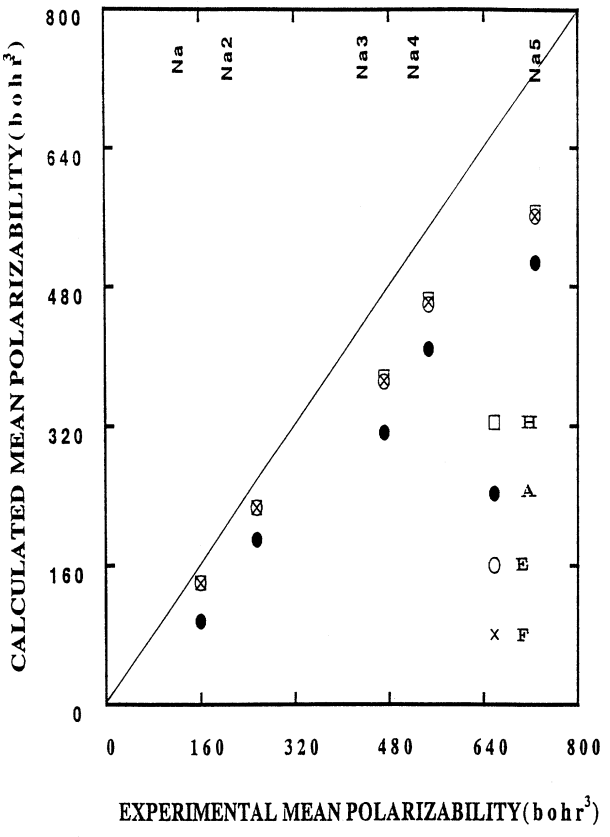

FIG. 2. Correlation plot of LDAxc mean polarizabilities versus experiment for various basis sets. The basis sets are described in Table II. Note that the points for basis sets E, F, and H essentially coincide and correspond to a higher mean polarizability than the points for basis set A. The origin of the slight odd-even alternation observed here with respect to the number of atoms in the cluster is not known, but may be related to differences between closed and open shell clusters.

Tables VI and VII show the effect of the choice of functional on the mean polarizability and polarizability anisotropy. Results for both the exchange-only and exchange-correlation functionals have been shown in order to allow a more complete analysis. Note that the effect of choice of functional on the polarizability anisotropy tends to be correlated with the effect on the

TABLE V. Sodium-cluster polarizability anisotropy calculated using the LDAxc approximation and various different basis sets at the LDAxc-optimized geometries. Here S and D refer to singlet and doublet, respectively.

	Polarizability anisotropy $\Delta\alpha$ (bohr^3)			
Basis[a]	Na_2 (S)	Na_3 (D)	Na_4 (S)	Na_5 (D)
A (DZVP)	190.97	289.48	516.19	495.40
B	117.22	271.62		
C	123.73	275.47		
D	137.93	294.06		
E (DZVP+)	135.82	284.58	446.44	430.86
F	135.63	284.74	447.90	431.96
G	190.74	290.58		
H	135.79	290.89	449.14	432.05

[a]See Table II.

mean polarizability in the sense that a functional which increases the mean polarizability tends to increase the polarizability anisotropy and vice versa. For this reason, we will focus our discussion on the mean polarizability.

Exchange and correlation are known to be treated differently in LDAxc calculations of polarizabilities than is the case in traditional *ab initio* theory.[68,69] This is partially a reflection of ambiguities in the definition of exchange in density-functional theory. (For example, should the exchange functionals in density-functional theory be designed to give the exchange energy associated with the Kohn-Sham orbitals or should they give the Hartree-Fock exchange energy?) Mean polarizabilities calculated at the LDAx level are larger than the corresponding Hartree-Fock quantities for rare gas atoms[68] and water,[69] but smaller for the sodium atom (Table VI) and comparable or slightly smaller for jellium sphere models of sodium clusters (Ref. 19, pp. 697–698). In contrast to the case with exchange, adding correlation by means of a local functional, to obtain the LDAxc results, always seems to lower the polarizability (Refs. 68 and 69 and Table VI). This has been explained by Stott and Zaremba[68] in terms of a competition between two effects. On the one hand, an admixture of excited-state configurations in the many-electron wave function tends to make the electron density more diffuse, hence increasing the polarizability. This is the dominant effect, beyond the Hartree-Fock level, on calculations of polarizabilities of rare gas atoms[68] and water.[69] On the other hand, electron correlation enhances the ability of the electrons to avoid each other, hence minimizing the effects of electron repulsions and leading to a more contracted charge density and smaller polarizabilities. This is the dominant effect, beyond the Hartree-Fock level, on calculations of

TABLE VI. Comparison of sodium-cluster mean polarizabilities calculated at the LDAxc-optimized geometries with experiment and with values obtained from other theoretical methods. The spin state is indicated in parentheses: S = singlet, D = doublet.

	Mean polarizability $\bar{\alpha}$ (bohr^3)					
Functional	Na (D)	Na_2 (S)	Na_3 (D)	Na_4 (S)	Na_5 (D)	Na_6 (S)
			Simple models			
Spillout[a]	159	269	371	468	562	654
			DFT with exchange-only functionals[b,c]			
LDAx	153.74	244.03	410.10	491.46	597.02	651.71
PW86x	129.00	225.45	387.54	465.11	564.72	622.08
B88x	158.27	247.42	425.84	498.51	607.08	660.60
			DFT with exchange-correlation functionals[b,c]			
LDAxc	140.12	226.24	371.27	459.17	560.02	611.64
PW86x+P86c	135.35	221.38	360.84	447.75	548.25	603.44
B88x+P86c	153.76	242.32	394.47	481.50	584.50	639.51
			DFT with effective core potentials			
BHS LDAxc[d]	141.7	223.3	363.0	452.8	587.7	603.2
brd LDAxc[d]	148.4	251.0	408.23	515.5	649.8	677.5
			Other theory			
HF[e]	190.9					
CEPA[f]	165.2					
MP4[g]		264.0				
EXPT[h]	159.27±3.37	255.78±8.10	471.06±16.20	545.97±20.25	726.16±29.02	823.89±30.36

[a]The value of the parameter $\delta = 1.43$ bohr was chosen to give the experimental mean polarizability for the atom.
[b]Present work.
[c]DZVP+ basis set. See Table II.
[d]ECP results from Ref. 21.
[e]Hartree-Fock (Ref. 25).
[f]Coupled-electron pair approximation (Ref. 27).
[g]Fourth-order Møller-Plesset many-body perturbation theory (Ref. 32).
[h]Calculated from the measurements of relative polarizabilities of Knight *et al.* (Ref. 4) and the absolute measurement of the atomic polarizability by Molof *et al.* (Ref. 26).

TABLE VII. Sodium-cluster polarizability anisotropy calculated with different exchange-correlation functionals at the LDAxc-optimized geometry.

	Polarizability anisotropy $\Delta\alpha$ (bohr^3)				
Functional	Na_2 (S)	Na_3 (D)	Na_4 (S)	Na_5 (D)	Na_6 (S)
DFT wth exchange-only functionals[a,b]					
LDAx	143.40	320.82	471.27	447.39	397.08
PW86x	148.22	311.79	465.70	437.65	389.05
B88x	145.56	341.49	478.43	457.16	403.51
DFT with exchange-correlation functionals[a,b]					
LDAxc	135.82	284.58	446.44	430.86	377.61
PW86x+P86c	139.78	272.37	444.22	424.42	379.89
B88x+P86c	139.03	301.07	461.76	440.50	391.56
DFT with effective core potentials					
BHS LDAxc[c]	142.4	260.5	382.1	339.4	318.88
Other theory					
MP4[d]	167				

[a]Present work.
[b]DZVP+ basis set. See Table II.
[c]ECP results from Ref. 21.
[d]Fourth-order Møller-Plesset many-body perturbation theory (Ref. 32).

the sodium atom polarizability (Table VI). It is also the dominant effect of the local-density correlation functional observed so far, regardless of the system.

Remarkably little is known about the effect of post-LDAxc functionals on the calculation of polarizabilities. In particular, little is known about whether and how knowledge gained for atoms[70] and small main group molecules[46,69,71] extends to metal clusters[21,12,72,14] (see also Ref. 19, pp. 697–698). What is known is that polarizabilities are sensitive to the asymptotic behavior of the effective potential and to "screening." This can be illustrated in terms of the well-known self-interaction error in the LDAxc. In the case of the atom, the self-interaction error means that the asymptotic behavior of the effective potential falls off exponentially fast rather than correctly as $1/r$ — that is, that the LDAx is less attractive than it should be at large r. This is consistent with the observation that Perdew-Zunger self-interaction corrections make the energies of occupied orbitals more negative.[73] Along the same lines, one might also think that self-interaction corrections would also lead to a less diffuse charge density and hence to smaller polarizabilities, and this too is consistent with previous observations that Perdew-Zunger self-interaction corrections tend to decrease polarizabilities.[21,70]

However, "screening" has an opposing effect on polarizabilities. The idea of screening is that the self-consistent field of electrons in a molecule reacts to an applied field in such a way as to reduce the effective field felt locally within the molecule. Since self-interaction errors lead to a self-consistent field which is too large in magnitude, they also lead to overscreening and hence to an overly small local field with decreased polarizing power. Thus, the effect of self-interaction errors on screening alone would be expected to *decrease* polarizabilities, while the effect on the orbital energies and asymptotic behavior of the effective potential should *increase* polarizabilities.[12] Which effect dominates in a given class of systems is difficult to say *a priori*. In the case of jellium spheres, at least some types of self-interaction corrections[12] and functionals with the correct asymptotic behavior[72,14] yield polarizabilities which are larger than those obtained in the LDA.

Returning to the effect of the present GCF's on calculated polarizabilities, we note that the rough agreement between the LDAx, B88x, and B88x+P86c mean polarizabilities in Table VI, and between the PW86x and PW86x+P86c in the same table, indicates, in the case of sodium clusters, that the P86c GCF tends to increase the mean polarizability in a manner which helps to compensate for the decrease caused by the LDA correlation functional. Thus the effect of the different GCF's on the mean polarizabilities of the sodium clusters can be largely explained in terms of just the exchange-only contributions to the GCF. For these, we note that the exchange-only GCF correction to the LDAx polarizability is opposite in sign for the PW86x and B88x GCF's.

There are remarkably few experimental measurements and good *ab initio* calculations of sodium-cluster polarizabilities with which we can compare our results. The available experimental measurements have been carried out in molecular beam experiments with static fields via either the E-H gradient balance method[74,26] or by direct measurement of the beam deflection in an applied electric field.[75–77,4] Although simple in principle, these experiments require careful analysis in order to obtain precise numbers.[26,75,77] This analysis yields mean polarizabilities but not polarizability anisotropies. The most reliable atomic measurement is the E-H gradient balance measurement of Molof *et al.*[26] Their number was used by Knight *et al.*[4] to calibrate their measurement of the mean polarizabilities of sodium clusters with up to 40 atoms. Reliable sodium-cluster polarizabilities from *ab initio* calculations are even rarer than are the experimental values. As mentioned in the Introduction, electron correlation effects have a significant impact on cal-

culated sodium-cluster polarizabilities, but ECP calculations which freeze the K and the L shells and thereby reduce sodium to what is effectively only a one-electron atom are unsuitable for inclusion of electron correlation effects. On the other hand, correlated calculations in which the L shell is left unfrozen exist only at the atomic level[27] and at the diatomic level.[32] In the case of the dimer, Sadlej and Urban[32] have completed calculations through fourth order in Møller-Plesset perturbation theory in which only the innermost (K) shell is frozen. No such calculations exist for clusters above the dimer.

Table VI shows our all-electron mean polarizabilities in comparison with experiment. For the atom and dimer, the LDAxc mean polarizabilities are about 12% too low compared to experiment. This difference jumps to 21% for the trimer, 16% for the tetramer, 23% for the pentamer, and 26% for the hexamer. The best gradient-corrected exchange-correlation functional to use for calculating the polarizability appears to be the B88x+P86c functional with errors of only 3.5% and 5.3%, respectively, for the atom and dimer. However, substantial discrepancies between theory and experiment still persist for the higher clusters: 16% for the trimer, 12% for the tetramer, 20% for the pentamer, and 22% for the hexamer. Our all-electron calculations can also be compared with the *ab initio* calculations of Reinsch and Meyer,[27] who obtained a mean polarizability of 165.2 bohr^3 for the atom using the coupled-electron pair approximation (CEPA) and with the *ab initio* calculations of Sadlej and Urban,[32] who obtained a mean polarizability for the dimer of 264 bohr^3 at the MP4 level. Since there are no measurements of polarizability anisotropies for sodium clusters, we can only compare our results for the dimer against that the MP4 result of Sadlej and Urban,[32] who obtained a value of 167 bohr^3. At first glance, this is relatively different from our calculated polarizability anisotropy. However, if reanalyzed in terms of the component along the bond and the component perpendicular to the bond, it is seen that the perpendicular component calculated at the B88x+P86c level (196 bohr^3) is in relatively good agreement with the perpendicular component of Sadlej and Urban (207 bohr^3) but that the B88x+P86c parallel component (335 bohr^3) is in less good agreement with that of Sadlej and Urban (375 bohr^3). Given the present level of agreement between theory and experiment, we have no idea whether this observation about parallel and perpendicular components is significant or just a coincidence.

The ECP LDAxc polarizabilities of Moullet and coworkers[21–24] have also been included in Tables VI and VII. In contrast to the case of optimized geometries, the LDAxc mean polarizabilities calculated using the *ab initio* BHS ECP are in better agreement with our all-electron LDAxc mean polarizabilities than are LDAxc mean polarizabilities calculated using the semiempirical brd ECP. Differences between the all-electron and BHS ECP mean polarizabilities range from about 1% for the atom to about 5% for the pentamer. In contrast, the brd ECP mean polarizabilities are in better agreement with experiment than are our B88x+P86c polarizabilities. Perhaps this is because the semiempirical brd ECP[67] involves dipole and quadrupole polarizability terms obtained from fitting the spectra of the atom. But this hardly explains why the brd ECP optimized geometries are in better agreement with our all-electron LDAxc geometries than were the BHS ECP optimized geometries.

Table VII shows that, unlike for the mean polarizabilities, the percent difference between our all-electron LDAxc polarizability anisotropies and those calculated with the *ab initio* BHS ECP is relatively large (5% for the dimer, 8% for the trimer, 14% for the tetramer, 21% for the pentamer, and 16% for the hexamer), as might be expected for such a sensitive property.

Mean polarizabilities calculated using the simple spill-out model have also been included in Table VI and are in remarkably good agreement with our all-electron LDAxc mean polarizabilities. We take this as more of a coincidence than anything else since these small clusters are hardly spherical.

C. Effect of small geometric distortions

One of the more remarkable things about the mean polarizabilities reported in the preceding subsection is the sudden jump in the discrepancy between theory and experiment in going from the dimer to the trimer. One hypothesis for why this might occur is that the trimer is the first cluster to have a floppy angular degree of freedom leading to somewhat larger errors in our optimized geometries. In order to investigate this hypothesis, we considered the effect of small geometric distortions on the mean polarizability and polarizability anisotropy.

Our analysis is aided by a few simple observations. The mean polarizability has units of volume and is, in fact, proportional to the volume of the sphere in the case of a classical metal sphere. An approximate relation between mean polarizability and volume has also been noted for molecules,[78] and a heuristic derivation of why this should be so is given in the Appendix. Thus some sort of "volume parameter" is a good choice when studying the geometry dependence of mean polarizabilities. In contrast, the formula for the polarizability anisotropy in the coordinate system which makes $\boldsymbol{\alpha}$ diagonal,

$$\Delta\alpha = \sqrt{\frac{(\alpha_{xx}-\alpha_{yy})^2 + (\alpha_{xx}-\alpha_{zz})^2 + (\alpha_{yy}-\alpha_{zz})^2}{2}} \tag{3.1}$$

makes it clear that it is a measure of the nonsphericity of the molecule.

Figure 3 shows the dependence of the mean polarizability and polarizability anisotropy of the dimer on its bond length. The graphs are remarkably linear over the range of these small distortions, so estimates of how these properties change with small distortions are easily made using the derivatives given in Table VIII. As noted above, our LDAxc bond length is 0.1 bohr too short in comparison with experiment. This 0.1 bohr uncertainty in the bond length corresponds to an uncertainty in the mean polarizability of 3.7 bohr^3 or about 1.4%, and an uncertainty

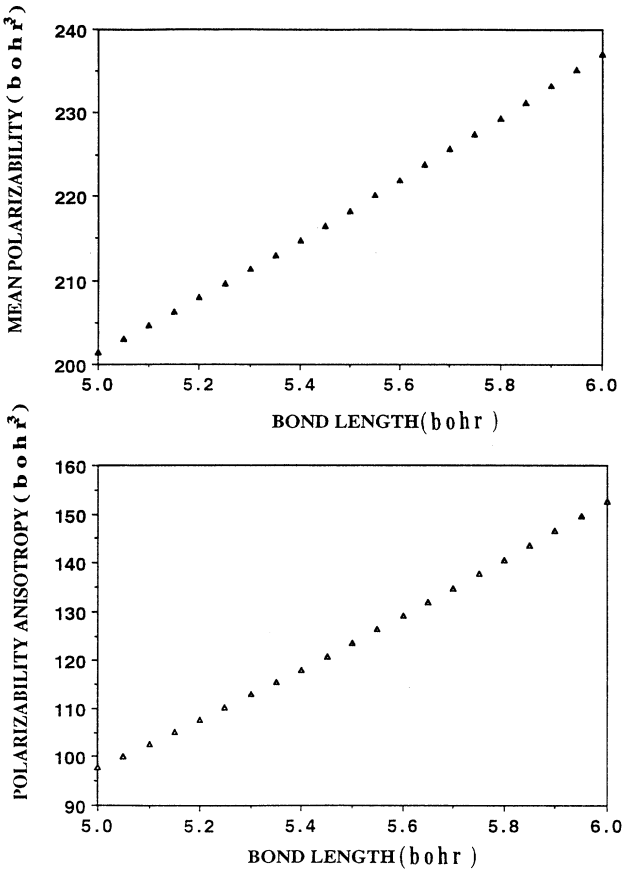

FIG. 3. Dependence of dimer mean polarizability and polarizability anisotropy on small changes in bond length.

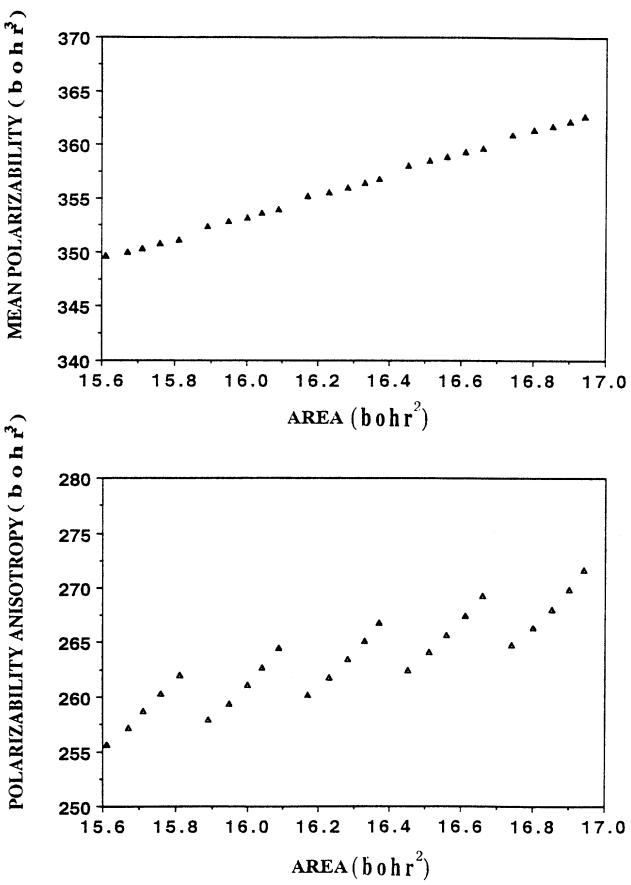

FIG. 4. Dependence of trimer mean polarizability and polarizability anisotropy on small changes in the area of the triangle formed by the three nuclei. C_{2v} symmetry is assumed and only the apex angle and the side length of the equilateral triangle are varied. The subsets of five points which are especially apparent in the graph for the polarizability anisotropy are an artifact of our sampling method. Each set corresponds to a single apex angle and a range of side lengths. See text for additional details.

in the polarizability anisotropy of 5.7 bohr^3 or about 4%. These numbers help to explain the observed 5.3% difference between the B88x+P86c mean polarizability of the dimer calculated at the LDAxc-optimized geometry and the experimental value.

On the other hand, the situation for the trimer is rather different. Figure 4 shows the dependence of the mean polarizability and polarizability anisotropy of the trimer on the area of the triangle formed by the three nuclei. As might be supposed from the volume argument above, the mean polarizability shows a remarkably linear dependence on this area while the polarizability anisotropy yields only a scatter plot when plotted against the triangle area. As shown in Table IV, there is a 4% difference between the area of our LDAxc-optimized structure and the area of the experimental structure. Based on the derivatives in Table VIII, this corresponds to an error in the mean polarizability of 7.6 bohr^3, or about 1.6%. That is, the anticipated error in the mean polarizability of the trimer is about the same as was the case for the dimer. This is hardly enough to account for the observed 16% discrepancy between the B88x+P86c mean polarizability and the experimental value.

These results emphasize the relative insensitivity of mean polarizabilities to small changes in geometry. At first this may seem to run counter to the commonly held belief that cluster polarizabilities yield information about cluster geometries. In fact, there is no contradiction. It is just that mean polarizabilities are sensitive to gross changes in geometries such as topological transitions between planar and three-dimensional structures, rather than the small differences likely to be encountered when the same structure is optimized using different theoretical methods.

TABLE VIII. Derivatives of polarizability with respect to bond length and bond angle for sodium dimer and trimer calculated at the LDAxc level.

Derivative	Na_2	Na_3
$\partial\bar{\alpha}/\partial R$ (bohr^2)	37.30	56.53
$\partial\Delta\alpha/\partial R$ (bohr^2)	57.45	45.89
$\partial\bar{\alpha}/\partial\phi$ (bohr^3/degree)		0.40
$\partial\Delta\alpha/\partial\phi$ (bohr^3/degree)		1.60
$\partial\bar{\alpha}/\partial A$ (bohr)		9.75

TABLE IX. Mean polarizabilities calculated at the B88x+P86c level for different topological structures. Structures labeled nA are the all-electron LDAxc-optimized structures of Na_n from Fig. 1. The other structures are those taken from the literature and shown in Fig. 5. The experimental mean polarizabilities are the same as those in Table VI.

Na_3		Na_4		Na_5		Na_6	
Structure	$\bar{\alpha}$ (bohr^3)	Structure	$\bar{\alpha}$ (bohr^3)	Structure	$\bar{\alpha}$ (bohr^3)	Strucuture	$\bar{\alpha}$ (bohr^3)
3A	394.47	4A	481.50	5A	584.50	6A	639.51
3B	546.13	4B	677.50	5B	763.32	6B	688.84
3C	385.69	4C	541.28	5C	809.48		
		4D	515.84	5D	606.60		
Average	442.10	Average	554.03	Average	690.98	Average	664.18
Expt.	471.06 ±16.20	Expt.	545.97 ±20.25	Expt.	726.16 ±29.02	Expt.	823.89 ±30.36

D. Other topologies

The analysis so far seems to indicate that the electronic polarizabilities of the clusters in their miniminum energy geometries are insufficient to account for the experimental polarizabilities of the trimer and higher-order clusters. Assuming that the measurements were performed on clusters in a reasonably equilibrated beam, this suggests that either zero-point motion is important or that there is sufficient thermal motion to sample other cluster configurations than the ones considered here so far. A crude estimate of the possible effect of molecular motion on the polarizability is made here by simply calculating the polarizability of alternative structures taken from the literature. These structures, not all of which are minima, are shown in Fig. 5. The corresponding polarizabilities are given in Table IX. A more rigorous study of the effects of molecular motion on the trimer polarizability is in progress.[79]

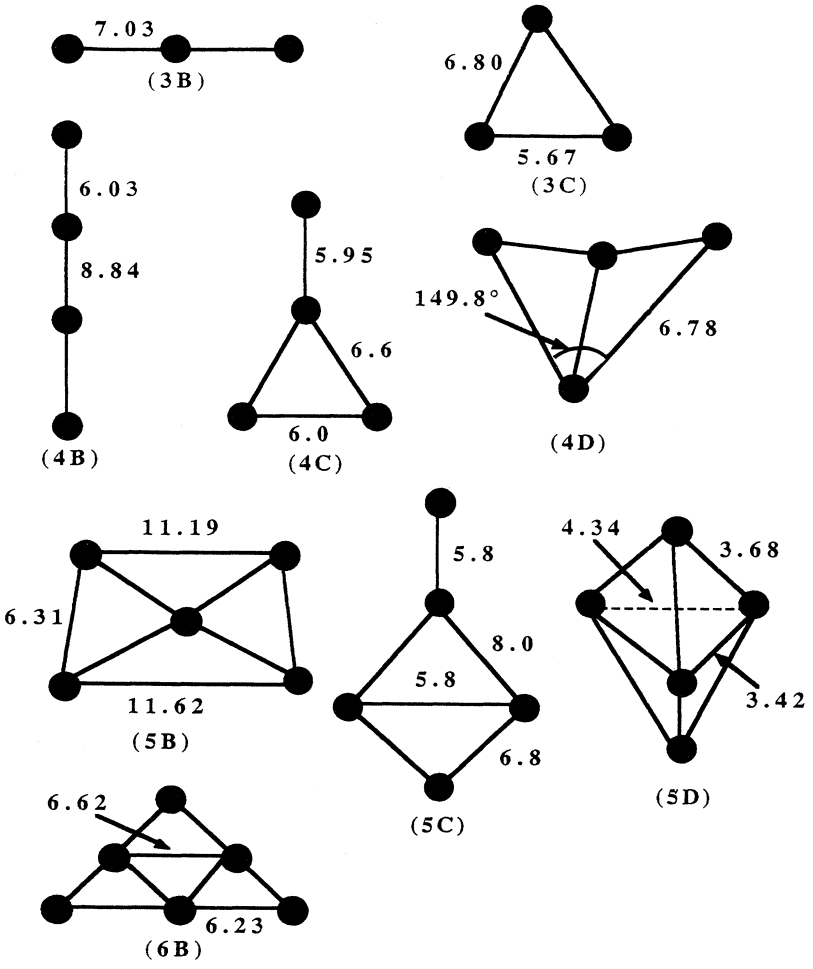

FIG. 5. Sodium cluster geometries used, together with structures from Fig. 1, for the calculations in Table IX. All structures are planar except for structures 4D and 5D, which are, respectively, a butterfly structure consisting of two equilateral triangles with a common edge and a distorted trigonal bipyramid. All internuclear distances are in bohr. Structures from Ref. 61 obtained from geometry optimizations using fourth-order Møller–Plesset perturbation theory: 3B ($D_{\infty h}$), 4B ($D_{\infty h}$), and 5B (C_{2v}). Structure from Ref. 22 obtained at the LDAxc level: 4C (C_{2v}). Structures from Ref. 59 obtained from Hartree-Fock approximation calculations: 4D (C_{2v}) and 5D (C_{2v}). Structure 5C (C_{2v}) from Ref. 81 obtained from the Hartree-Fock approximation plus a density-functional correction for electron correlation. Structure 3C (C_{2v}) was optimized for the present work at the all-electron LDAxc/DZVP level and was found to be 1.8 mhartree higher than the corresponding obtuse structure from Fig. 1 when treated at the same level. Structure 6B (D_{3h}) was optimized for the present work at the all-electron LDAxc/DZVP level and was found to be 1.9 mhartree higher than the corresponding C_{5v} structure from Fig. 1 when treated at the same level.

Our conclusions can be best illustrated by concentrating on the trimer for the moment. The sodium trimer potential energy surface[79] has minima corresponding to the obtuse triangle of Fig. 1 and transition states corresponding to the acute triangle and linear structure of Fig. 5. The calculated polarizabilities of the triangular structures are each around 390 bohr^3, which is significantly below the experimentally observed value of 471.06 bohr^3. However, the calculated polarizability of the linear structure is 546 bohr^3, which exceeds the experimental value. Since the linear transition state lies at the top of a long low barrier,[79] the measured polarizability might be explained by the trimer spending a significant time in a nearly linear structure as it interconverts between minima. It is interesting to note, in this regard, that a strong tendency towards sampling the linear configuration has been found by Liu, Carter, and Carter in their recent *ab initio* molecular dynamics calculations.[80] In fact, assuming that the clusters are fluxional under the conditions at which the polarizability is measured allows us to make a crude estimate (Table IX) of the experimental polarizability simply by averaging the polarizabilities obtained at several different cluster geometries. The agreement with experiment is, in fact, remarkably good for all but the hexamer, suggesting that molecular motion may be an important factor in explaining the experimental polarizabilities, although a more rigorous treatment of molecular motion effects is certainly desirable.[79]

IV. CONCLUSION

All-electron local and gradient-corrected density-functional calculations of geometries and polarizabilities have been performed for sodium clusters through the hexamer. Such calculations are useful for the developing and testing of effective core potentials with applications to larger clusters in mind, and this use of all-electron calculations has been illustrated here by comparing our LDAxc results with LDAxc results from the literature obtained using ECP's. The results reported in this paper are currently being used in our laboratory to assess and improve new model core potentials for studying the optical properties of much larger clusters.

However, a more fundamental use of our all-electron results is in benchmarking density-functional theory. To this end, calculations of polarizabilities have been performed with both local and gradient-corrected functionals and compared against the available data from experimental measurements and high-quality *ab initio* calculations. Based on this comparison, we find that, of all the functionals tested, the Becke 1988 exchange plus Perdew 1986 correlation gradient-corrected functionals give the mean polarizabilities in best agreement with the experimental quantities. In particular, discrepancies for the atomic and diatomic mean polarizabilities are only 3.5% and 5%, respectively. The discrepancy between theory and experiment increases to between 11% and 22% for the higher clusters.

A 20% discrepancy between sodium-cluster LDAxc mean polarizabilities calculated with the jellium sphere model and experimental sodium-cluster mean polarizabilities has been remarked before.[12,72] The existence of a similar discrepancy between our molecular calculations and experiment suggests that the problem may not be an artifact of the jellium sphere model.

In fact, we find it difficult to explain the increased discrepancy between theory and experiment for clusters higher than the dimer in terms of errors in the calculated electronic polarizability. Our basis sets (both orbital and auxiliary) appear to be quite adequate for the properties we are calculating. We have shown that the changes cannot be explained from small errors in geometries. And finally, it is difficult to understand why a functional which works well for calculating the polarizability of the atom and dimer should work significantly less well for higher-order clusters.

To emphasize this point, we have reoptimized the geometries of the dimer and trimer using the best basis set in Table II (basis H) and the B88x+P86c GCF and then recalculated the polarizabilities at these geometries with this basis and functional. The reoptimized geometries (given in Tables III and IV) are essentially identical to those obtained at the B88x+P86c/DVZP+ level. The resultant mean polarizabilities are 247.51 bohr^3 and 413.33 bohr^3, respectively, for the dimer and trimer. As expected, this level of calculation does reduce the discrepancy between the experimental and calculated polarizabilities (to 3% for the dimer and 12% for the trimer), but the large jump in the level of agreement between theory and experiment in going from the dimer to the trimer remains.

This leads us to suggest that some of the missing 20% is likely to be a real difference between the static electronic polarizability at the minimum energy geometry and the experimentally measured quantity. We suggest that molecular motion effects may need to be taken into account before a completely satisfactory explanation of the experimental polarizabilities can be given. In particular, it is worthwhile remembering that the *E-H* gradient balance and beam deflection experiments are carried out with static electric fields and in principle measure a quantity with orientational and vibrational as well as electronic components. The orientational component and vibrational correction to the zero point average of the electronic polarizability are not zero unless the dipole moment of the molecule is zero[77,21] and both act to increase the polarizability. Although small, the dipoles are not zero for the geometries of Na_3, Na_5, and Na_6 considered here. Finite temperature effects will lead to further contributions from molecular motion. Some attempt has been made to model these by simply averaging polarizabilities calculated at different geometries taken from the literature. This crude but suggestive estimate gives remarkably good agreement with the experimentally observed polarizabilities. However, work is in progress[79] to give a more rigorous estimate of the effects of molecular motion on the polarizability.

ACKNOWLEDGMENTS

This study grew out of discussions with the late Professor Michael Dignam. Professors Andrzej Sadlej and Mi-

raslav Urban are thanked for making their results available to us prior to publication. We would also like to thank Sebastien Lefebvre and Professor Tucker Carrington for useful discussions regarding the dynamics of Na_3. Financial support from the Canadian Network of Centres of Excellence in Molecular and Interfacial Dynamics (CEMAID) is gratefully acknowledged.

APPENDIX: AVERAGE ENERGY AND INDEPENDENT PARTICLE APPROXIMATION

A very rough approximation is derived here in which the mean polarizability appears as the sum of orbital terms which are functions of both the "size" of the orbital and an average excitation energy. We will focus on calculating α_{xy}, but extension to the other components of $\boldsymbol{\alpha}$ will be clear.

We begin by deriving an exact sum-over-states expression. Introducing an electric field term FY in the Hamiltonian, where

$$Y = \sum_{i=1}^{N} y(i)\,, \tag{A1}$$

results in the N-electron wave function

$$\Psi_0(F) = \Psi_0 + F\delta\Psi_0 + O(F^2)\,, \tag{A2}$$

where, by elementary Rayleigh-Schrödinger perturbation theory,

$$\delta\Psi_0 = \sum_{I}^{I\neq 0} \Psi_I \frac{\langle\Psi_I|Y|\Psi_0\rangle}{E_0 - E_I}\,. \tag{A3}$$

The electronic component of the dipole moment in the presence of the field is

$$\mu_x(F) = -\langle\Psi_0(F)|X|\Psi_0(F)\rangle\,, \tag{A4}$$

where

$$X = \sum_{i=1}^{N} x(i)\,. \tag{A5}$$

Since

$$\alpha_{xy} = \left(\frac{\partial\mu_x(F)}{\partial F}\right)_{F=0}\,, \tag{A6}$$

then

$$\alpha_{xy} = -2\mathrm{Re}\langle\Psi_0|X|\delta\Psi_0\rangle\,. \tag{A7}$$

Substituting in Eq. (A3) gives the sum-over-states expression

$$\alpha_{xy} = -2\sum_{I}^{I\neq 0} \frac{\mathrm{Re}\left(\langle\Psi_0|X|\Psi_I\rangle\langle\Psi_I|Y|\Psi_0\rangle\right)}{E_0 - E_I}\,. \tag{A8}$$

No approximations have been made up to this point other than the usual Born-Oppenheimer separation of electronic and nuclear degrees of freedom. However, in the absence of accurate many-electron wave functions Ψ_I and their corresponding energies E_I, approximate wave functions and energies need to be introduced before the sum-over-states formula can become computationally useful. We do this by making the *assumption* that Ψ_0 can be approximated by a single determinant wave function Φ, and that the Ψ_I can be approximated by singly excited determinants Φ_i^a, doubly excited determiants Φ_{ij}^{ab}, etc. It is also convenient to relabel the corresponding energies with orbital indices (e.g., $E_I \rightarrow E_{ij}^{ab}$). Substituting these determinants into the sum-over-states expression and taking into account the vanishing of matrix elements $\langle\Phi|X|\Phi_{ij\ldots}^{ab\cdots}\rangle$ involving higher-than-single excitations gives

$$\alpha_{xy} = -2\sum_{i}^{\text{occupied}}\sum_{a}^{\text{virtual}} \frac{\mathrm{Re}\left(\langle\Phi|X|\Phi_i^a\rangle\langle\Phi_i^a|Y|\Phi\rangle\right)}{E_0 - E_i^a}\,. \tag{A9}$$

Evaluating the integrals gives the orbital expression

$$\alpha_{xy} = -2\sum_{i}^{\text{occupied}}\sum_{a}^{\text{virtual}} \frac{\mathrm{Re}\left(\langle\psi_i|x|\psi_a\rangle\langle\psi_a|y|\psi_i\rangle\right)}{E_0 - E_i^a} \tag{A10}$$

or

$$\alpha_{xy} = +2\sum_{i}^{\text{occupied}}\sum_{p}^{p\neq i} \frac{\mathrm{Re}\left(\langle\psi_i|x|\psi_p\rangle\langle\psi_p|y|\psi_i\rangle\right)}{\Delta E_i^p}\,, \tag{A11}$$

where

$$\Delta E_i^p = \begin{cases} E_i^p - E_0; & p \text{ virtual} \\ -\Delta E_p^i; & p \text{ occupied.} \end{cases} \tag{A12}$$

This last definition is motivated by the independent particle picture where the excitation energy is a difference of orbital energies,

$$\Delta E_i^p = \epsilon_p - \epsilon_i\,; \tag{A13}$$

however, the exact definition of the "occupied-to-occupied orbital excitation energy" is not critical since these terms cancel out in Eq. (A11).

We now make one more approximation in addition to the quasi-independent particle approximation made up to this point. Specifically, we make the average energy approximation, which consists of replacing the excitation energies ΔE_i^p with an average excitation energy ΔE_i^{avg}, out of each orbital i. (Admittedly, the choice of occupied-to-occupied orbital exciation energy may be more important here, but the approximations are rough and we can always fall back on the difference of orbital energies.) With this approximation, and using the completeness relation,

$$\sum_{i}^{p\neq i} |\psi_p\rangle\langle\psi_p| = \hat{1} - |\psi_i\rangle\langle\psi_i|\,, \tag{A14}$$

Eq. (A11) becomes

$$\alpha_{xy} = 2 \sum_{i}^{\text{occupied}} \frac{\langle xy \rangle_i - \langle x \rangle_i \langle y \rangle_i}{\Delta E_i^{\text{avg}}}, \tag{A15}$$

where $\langle\rangle_i$ stand for the expectation value taken with respect to the orbital ψ_i. At this level of approximation, the mean polarizability is just

$$\bar{\alpha} = \frac{2}{3} \sum_{i}^{\text{occupied}} \frac{\langle |\vec{r}|^2 \rangle_i - |\langle \vec{r} \rangle_i|^2}{\Delta E_i^{\text{avg}}}, \tag{A16}$$

which shows the relationship between the size of the orbital charge clouds and the mean polarizability.

[1] H.C. van de Hulst, *Light Scattering by Small Particles* (Dover, New York, 1981).
[2] J.A.A.J. Perenboom, P. Wyder, and F. Meier, Phys. Rep. **78**, 173 (1981).
[3] R. Siegel, Phys. Today **46** (10), 64 (1993).
[4] W.D. Knight, K. Clemenger, W.A. de Heer, and W.A. Saunders, Phys. Rev. B **31**, 2539 (1985).
[5] W.A. de Heer, P. Milani, and A. Châtelain, Phys. Rev. Lett. **63**, 2834 (1989).
[6] P. Milani, I. Moullet, and W.A. de Heer, Phys. Rev. A **42**, 5150 (1990).
[7] C.J.F. Böttcher, *Theory of Electronic Polarization. I. Dielectrics in Static Fields* (Elsevier, New York, 1973), p. 86.
[8] C. Kittel, *Introduction to Solid State Physics*, 3rd ed. (John Wiley and Sons Inc., New York, 1967).
[9] D.E. Beck, Phys. Rev. B **30**, 6935 (1984).
[10] M.J. Puska, R.M. Nieminen, and M. Manninen, Phys. Rev. B **31**, 3486 (1985).
[11] M. Manninen, R.M. Nieminen, and M.J. Puska, Phys. Rev. B **33**, 4289 (1986).
[12] P. Stampfli and K.H. Bennemann, Phys. Rev. A **39**, 1007 (1989).
[13] A. Dellafiore and F. Matera, Phys. Rev. B **41**, 3488 (1990).
[14] A. Rubio, L.C. Balbás, and J.A. Alonso, Phys. Rev. B **46**, 4891 (1992).
[15] A. Rubio, L.C. Balbás, and J.A. Alonso, Phys. Rev. B **45**, 13 657 (1992).
[16] P. Joyes, *Les agrégats Inorganiques Élémentaires* (Les Éditions de Physique, Les Ulis Cedex, France, 1990).
[17] W.D. Knight, W.A. de Heer, W.A. Saunders, M.Y. Chou, and M.L. Cohen, Phys. Rev. Lett. **52**, 2141 (1984).
[18] W.A. de Heer, Rev. Mod. Phys. **65**, 611 (1993).
[19] M. Brack, Rev. Mod. Phys. **65**, 677 (1993).
[20] M. Manninen, Phys. Rev. B **34**, 6886 (1986).
[21] I. Moullet, Ph.D. thesis, Ecole Polytechnique Féderale de Lausanne, 1989.
[22] I. Moullet, J.L. Martins, F. Reuse, and J. Buttet, Phys. Rev. Lett. **65**, 476 (1990).
[23] I. Moullet, J.L. Martins, F. Reuse, and J. Buttet, Phys. Rev. B **19**, 31 (1990).
[24] I. Moullet, J.L. Martins, F. Reuse, and J. Buttet, Z. Phys. D **12**, 353 (1989).
[25] A.J. Sadlej and M. Urban, J. Mol. Struct. (Theochem) **234**, 147 (1991).
[26] R.W. Molof, H.L. Schwartz, T.M. Miller, and B. Bederson, Phys. Rev. A **10**, 1131 (1974).
[27] E.A. Reinsch and W. Meyer, Phys. Rev. A **14**, 915 (1976).
[28] G. Figari, G.F. Musso, and V. Magnasco, Mol. Phys. **50**, 1173 (1983).
[29] P.-O. Widmark, B. Joakim, Persson, and B.O. Roos, Theor. Chem. Acta **79**, 419 (1991).
[30] W. Müller and W. Meyer, J. Chem. Phys. **85**, 953 (1986).
[31] J. Flad, G. Igel, M. Dolg, H. Stoll, and H. Preuss, Chem. Phys. **75**, 331 (1983).
[32] A.J. Sadlej and M. Urban (private communication).
[33] W. Kohn and L.J. Sham, Phys. Rev. **140**, A1133 (1965).
[34] R.G. Parr and W. Yang, *Density-Functional Theory of Atoms and Molecules* (Oxford University Press, New York, 1989).
[35] R.M. Dreizler and E.K.U. Gross, *Density Functional Theory* (Springer-Verlag, New York, 1990).
[36] N.H. March, *Electron Density Theory of Atoms and Molecules* (Academic Press, New York, 1992).
[37] deMon is based on a program written by Alain St-Amant at l'Université de Montréal between 1988 and 1991 under the direction of Professor Dennis R. Salahub.
[38] S.H. Vosko, L. Wilk, and M. Nusair, Can. J. Phys. **58**, 1200 (1980).
[39] D.M. Ceperley and B.J. Alder, Phys. Rev. Lett. **45**, 566 (1980).
[40] A.D. Becke, Phys. Rev. A **38**, 3098 (1988).
[41] J.P. Perdew and Y. Wang, Phys. Rev. B **33**, 8800 (1986).
[42] J.P. Perdew, Phys. Rev. B **33**, 8822 (1986).
[43] D.C. Langreth and M.J. Mehl, Phys. Rev. B **28**, 1809 (1983).
[44] E.R. Davidson and D. Feller, Chem. Rev. **86**, 681 (1986).
[45] J. Guan, P. Duffy, J.T. Carter, D.P. Chong, K.C. Casida, M.E. Casida, and M. Wrinn, J. Chem. Phys. **98**, 4753 (1993).
[46] F. Sim, D.R. Salahub, and S. Chin, Int. J. Quantum Chem. **43**, 463 (1992).
[47] G.D. Zeiss, W.R. Scott, N. Suzuki, D.P. Chong, and S.R. Langhoff, Mol. Phys. **37**, 1543 (1979).
[48] J.L. Dodds, R. McWeeny, and A.J. Sadlej, Mol. Phys. **34**, 1779 (1977).
[49] A.J. Sadlej, Chem. Phys. Lett. **47**, 50 (1977).
[50] A.J. Sadlej, Mol. Phys. **34**, 855 (1977).
[51] M.A. Spackman, J. Phys. Chem. **93**, 7594 (1989).
[52] H.-J. Werner and W. Meyer, Mol. Phys. **31**, 855 (1976).
[53] J.L. Martins, J. Buttet, and R. Car, Phys. Rev. B **31**, 1804 (1985).
[54] A.D. Becke, Phys. Rev. A **33**, 2786 (1986).
[55] D. Heinemann and A. Rosén, Theor. Chim. Acta **85**, 249 (1993).
[56] T.L. Cottrell, *The Strengths of Chemical Bonds*, 2nd ed. (Butterworths, London, 1958).
[57] K.K. Vrma, J.T. Bahns, A.R. Rejei-Rizi, W.C. Stwalley, and W.T. Zemke, J. Chem. Phys. **78**, 3599 (1983).
[58] H.-A. Eckel, J.-M. Gress, J. Biele, and W. Demtröder, J. Chem. Phys. **98**, 135 (1992).
[59] V. Bonačić-Koutecký, P. Fantucci, and J. Koutecký, Phys. Rev. B **37**, 4369 (1988).
[60] F. Spieglmann and D. Pavolini, J. Chem. Phys. **89**, 4954 (1988).
[61] A.K. Ray, Solid State Commun. **71**, 311 (1989).
[62] V. Bonačić-Koutecký, P. Fantucci, and J. Koutecký, Chem.

Rev. **91**, 1035 (1991).
[63] V. Bonačić-Koutecký, P. Fantucci, and J. Koutecký, J. Chem. Phys. **93**, 3802 (1990).
[64] H.-O. Beckmann, J. Koutecký, and V. Bonačić-Koutecký, J. Chem. Phys. **73**, 5182 (1980).
[65] R.L. Martins and E.R. Davidson, Mol. Phys. **35**, 1713 (1978).
[66] G.B. Bachelet, D.R. Hamann, and M. Schlüter, Phys. Rev. B **26**, 4199 (1982).
[67] J.N. Bardsley, Case Stud. At. Phys. **4**, 299 (1974).
[68] M.J. Stott and E. Zaremba, Phys. Rev. A **21**, 12 (1980).
[69] P. Duffy, D.P. Chong, M.E. Casida, and D.R. Salahub, Phys. Rev. A **50**, 4707 (1994).
[70] G.D. Mahan and K.R. Subbaswamy, *Local Density Theory of Polarizability* (Plenum Press, New York, 1990).
[71] A.M. Lee and S.M. Colwell, J. Chem. Phys. **101**, 9704 (1994).
[72] A. Rubio, L.C. Balbás, Ll. Serra, and M. Barranco, Phys. Rev. B **42**, 1095 (1990).
[73] J.P. Perdew and A. Zunger, Phys. Rev. B **23**, 5048 (1981).
[74] A. Salop, E. Pollack, and B. Bederson, Phys. Rev. **124**, 1431 (1961).
[75] W.D. Hall and J.C. Zorn, Phys. Rev. A **10**, 1141 (1974).
[76] R.W. Molof, T.M. Miller, H.L. Schwarz, B. Benderson, and J.T. Park, J. Chem. Phys. **61**, 1816 (1974).
[77] V. Tarnovsky, M. Bunimovicz, L. Vušković, B. Stumpf, and B. Benderson, J. Chem. Phys. **98**, 3894 (1993).
[78] T. Brinck, J.S. Murray, and P. Politzer, J. Chem. Phys. **98**, 4305 (1993).
[79] S. Lefevre, T. Carrington, J. Guan, M.E. Casida, and D.R. Salahub (unpublished).
[80] Z. Liu, L.E. Carter, and E.A. Carter, J. Phys. Chem. **99**, 4355 (1995).
[81] J. Flad, H. Stoll, and H. Preuss, J. Chem. Phys. **71**, 3042 (1979).